Weighted Generalised Procrustes Analysis of Diffusion Tensors

Diwei Zhou[1], Ian L. Dryden[1,2], Alexey Koloydenko[3] and Li Bai[4]

[1] School of Mathematical Sciences, University of Nottingham
[2] Department of Statistics, University of South Carolina
[3] Department of Mathematics, Royal Holloway, University of London
[4] School of Computer Science, University of Nottingham

1 Introduction

Diffusion tensor imaging (DTI) is a specific MRI modality which provides a unique insight into tissue structure and organisation *in vivo*. In DTI, displacement of water molecules over time is modelled by a zero-mean trivariate Gaussian distribution (Alexander, 2005) with covariance matrix evolving linearly with time and determined by the diffusion tensor (DT), a 3×3 symmetric positive-definite matrix. DT inference from observed diffusion MRI data has been commonly carried out using least squares (Koay *et al.*, 2006) and Bayesian (Behrens *et al.*, 2007, Zhou *et al.*, 2008) methods. At each location (voxel) of interest, the principal eigenvector of the tensor estimates the dominant fibre orientation whereas various tensor-derived diffusion anisotropy indices measure local anisotropy. White matter tractography attempts to integrate local estimates into brain connectivity maps which are of interest in neuroscience. In particular, DTI has been used to study stroke (Le Bihan *et al.*, 2001) and a wide range of neurological disorders such as multiple sclerosis, Alzheimer's and Parkinson's disease, and schizophrenia (Lenglet *et al.*, 2009).

Since diffusion MRI is a relatively low resolution modality, advanced tensor processing methods such as non-Euclidean interpolation, have been considered. Yet, reliable and accurate estimation of the highly complex white matter architecture of the brain remains a challenge despite the many advances in modelling, processing, and analysis of diffusion MRI data (Lenglet *et al.*, 2009). Moreover, further inference, e.g. analysis of variance across groups, depends critically on tensor processing methods such as interpolation (Chao *et al.*, 2008). At the same time, the recently introduced DT processing methods based on Procrustes analysis (Dryden *et al.*, 2009) have shown promising performance and deserve further investigation. Thus, this paper explores *weighted generalized Procrustes analysis (WGPA)* in which an arbitrary number of tensors can be interpolated or smoothed efficiently with the additional flexibility of controlling their individual contributions. The approach is illustrated through synthetic examples as well as white matter tractography of a healthy human brain.

2 Weighted Generalised Procrustes Analysis

Now consider a sample of N DT's $\mathbf{D}_1$, ..., $\mathbf{D}_N$. To ensure the positive definiteness of DT's, a reparameterization is used, i.e., $\mathbf{D}_i = \mathbf{Q}_i\mathbf{Q}_i^T$, where $\mathbf{Q}_i \in \mathbb{R}^{3\times3}$. For example, $\mathbf{Q}_i = chol(\mathbf{D}_i)$ is the *Cholesky decomposition*, where $\mathbf{Q}_i$ is lower triangular with positive diagonal elements. Note that $\mathbf{Q}_i$ and any rotation and reflection of it $\mathbf{Q}_i\mathbf{R}_i$ ($\mathbf{R}_i \in O(3)$) can result in the same $\mathbf{D}_i$, i.e. $\mathbf{D}_i = \mathbf{Q}_i\mathbf{Q}_i^T = \mathbf{Q}_i\mathbf{R}_i(\mathbf{Q}_i\mathbf{R}_i)^T, i = 1, ..., N$.

The weighted Fréchet sample mean of $\mathbf{D}_1$, ..., $\mathbf{D}_N$ at N voxels with a certain distance function dist is defined by:

$$\bar{\mathbf{D}} \;=\; \arg\inf_{\mathbf{D}} \sum_{i=1}^{N} w_i \mathrm{dist}(\mathbf{D}_i, \mathbf{D})^2, \tag{1}$$

where the weights w_i are proportional to a function of the Euclidean distance between locations of the tensors (voxels), $0 \leq w_i \leq 1$ and $\sum_{i=1}^{N} w_i = 1$.

Weighted generalized Procrustes analysis (WGPA) is proposed to obtain the weighted mean of $\mathbf{D}_1$, ..., $\mathbf{D}_N$. The objective of WGPA under rotation and reflection is to minimise a sum of weighted squared Euclidean norms S_{WGPA} which is given by

$$\begin{aligned} S_{WGPA}(\mathbf{D}_1, ..., \mathbf{D}_N) &= \inf_{\mathbf{R}_1,...,\mathbf{R}_N} \sum_{i=1}^{N} w_i \parallel \mathbf{Q}_i\mathbf{R}_i - \sum_{j=1}^{n} w_j \mathbf{Q}_j \mathbf{R}_j \parallel^2 \\ &= \inf_{\mathbf{R}_1,...,\mathbf{R}_N} \sum_{i=1}^{N} w_i \parallel (1-w_i)\mathbf{Q}_i\mathbf{R}_i - \sum_{j\neq i} w_j \mathbf{Q}_j \mathbf{R}_j \parallel^2 \\ &= \inf_{\mathbf{R}_1,...,\mathbf{R}_N} \sum_{i=1}^{n} \frac{w_i}{(1-w_i)^2} \parallel \mathbf{Q}_i\mathbf{R}_i - \frac{1}{(1-w_i)} \sum_{j\neq i} w_j \mathbf{Q}_j \mathbf{R}_j \parallel^2 . \end{aligned} \tag{2}$$

Let $\hat{\mathbf{R}}_i, i = 1, ..., N$ be the estimates of the rotation matrices. Then, the *WGPA mean tensor* is given by

$$\bar{\mathbf{D}}_{WGPA} = \bar{\mathbf{Q}}_{WGPA} \bar{\mathbf{Q}}_{WGPA}^T, \tag{3}$$

where $\bar{\mathbf{Q}}_{WGPA} = \sum_{i=1}^{N} w_i \mathbf{Q}_i \hat{\mathbf{R}}_i$. We give Algorithm 1 for estimating $\hat{\mathbf{R}}_i, i = 1, ..., N$.

Algorithm 1 Weighted Generalised Procrustes Method

Initial setting: $Q_i^P \leftarrow chol(D_i), i = 1, ..., N$
S_{WGPA} from previous iteration: $S_p \leftarrow 0$
S_{WGPA} from current iteration: $S_c \leftarrow \sum_{i=1}^{N} w_i \parallel Q_i^P - \sum_{j=1}^{N} w_j Q_j^P \parallel^2$
while $|S_p - S_c| >$ tolerance **do**
  for $i = 1$ to N **do**
    $\bar{Q}_i = \frac{1}{1-w_i} \sum_{j\neq i} w_j Q_j^P$
    Calculate the rotation matrix R_i which minimises $\parallel \bar{Q}_i - Q_i^P R_i \parallel$ with partial ordinary Procrustes analysis
    $Q_i^P \leftarrow Q_i^P R_i$
  end for
  $S_p \leftarrow S_c$
  $S_c \leftarrow \sum_{i=1}^{N} w_i \parallel Q_i^P - \sum_{j=1}^{N} w_j Q_j^P \parallel^2$
end while
$\bar{Q}_{WGPA} \leftarrow \sum_{i=1}^{N} w_i Q_i^P$
return $\bar{Q}_{WGPA}$

3 Results

3.1 Geodesic interpolation

Figure 1 presents geodesic interpolations of two synthetic DT's (in red) with Euclidean (d_E), Procrustes (d_S), Log-Euclidean (d_L) and Riemannian (d_R) metrics repectively. There is a clear swelling effect in Euclidean case. However, Procrustes, Log-Euclidean and Riemannian means provide more reasonable interpolations.

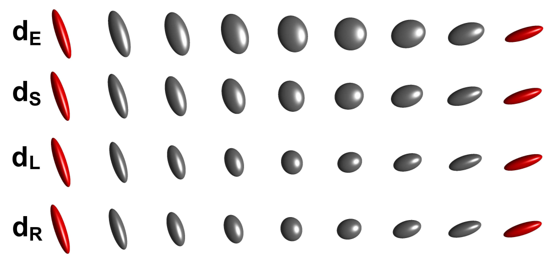

Figure 1: Geodesic interpolations between two anisotropic diffusion tensors (in red) with Euclidean d_E, Procrustes d_S, Log-Euclidean d_L and Riemannian d_R methods from top to bottom.

3.2 Applications to real data

A tensor field from a healthy human brain has been smoothed and interpolated (with 2 interpolations between each pair of original voxels). The Fractional Anisotropy (FA) maps from the processed tensors are shown in Figure 2. Obviously, the FA map from the processed tensor data is much smoother than the one without processing. The feature that the cingulum is distinct from the corpus callosum is clearer in the anisotropy map from the processed data than those without processing in Figure 2.

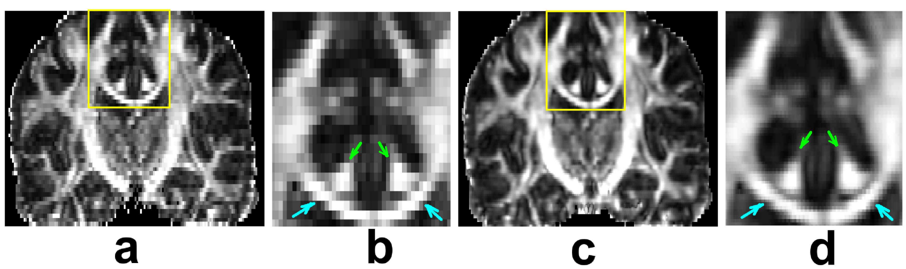

Figure 2: Smoothing and interpolation of the diffusion tensor data from human brain. a: FA map from Bayesian tensor field. c: FA map from processed tensor field. b and d: Zoomed inset regions. Green arrows: the cingulum. Light blue arrows: the corpus callosum.

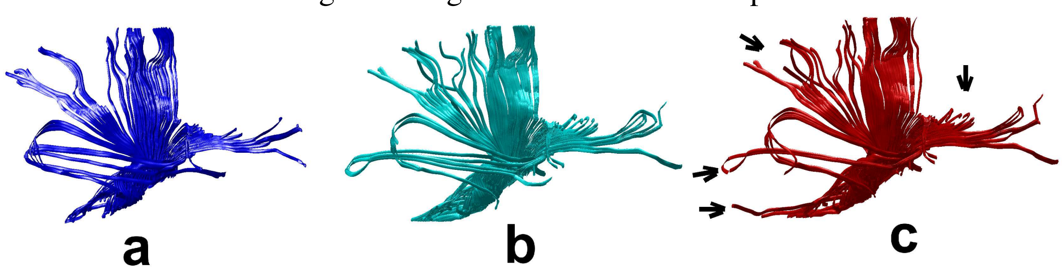

Figure 3: Fibre tractograhpies using the Bayesian estimates (a), Euclidean smoothing (b) and WGPA smoothing (c). Black arrows point out some obvious differences of the WGPA tracts compared with other methods.

Initial results of fibre tractographies of the brain stem in a healthy human brain have been shown in Figure 3. Tractography from WGPA processed tensor field is different from the other methods, and work is currently underway to assess whether WGPA is preferable.

References

Alexander, D. C. (2005). Multiple-fibre reconstruction algorithms for diffusion MRI. *Annals of the New York Academy of Sciences*, 1046:113–133.

Chao, Tzu-Cheng, Chou, Ming-Chung, Yang, Pinchen, Chung, Hsiao-Wen, Wu, Ming-Ting. (2008). Effects of interpolation methods in spatial normalization of diffusion tensor imaging data on group comparison of fractional anisotropy. Magnetic resonance imaging. In press.

Dryden, I. and Mardia, K. (1998). *Statistical Shape Analysis*. Wiley & Sons, Chichester.

Dryden, I.L., Koloydenko, A. and Zhou, D. (2009). Non-Euclidean statistics for covariance matrices, with applications to diffusion tensor imaging. To appear: *Annals of Applied Statistics*.

Behrens, T. E. J, Johansen-Berg H., Jbabdi S., Rushworth M. F. S., Woolrich M. W. (2007). Probabilistic diffusion tractography with multiple fibre orientations. What can we gain? *Neuroimage*, 34(1):144–55.

Koay, C. G., Carew, J. D., Alexander, A. L., Basser, P. J., and Meyerand, M. E. (2006). Investigation of anomalous estimates of tensor-derived quantities in diffusion tensor imaging. *Magnetic Resonance in Medicine* , 55:930–936.

Le Bihan, D., Mangin, J. F., Poupon, C., Clark, C. A., Pappata, S., Molko, N., and Chabriat, H. (2001). Diffusion tensor imaging: concepts and applications. *Journal of Magnetic Resonance Imaging*, 13:534–546.

Lenglet, C., Campbell, J. S. W., Descoteaux, M., Haro G., Savadjiev, P., Wassermann, D., Anwander, A., Deriche, R., Pike, G. B., Sapiro, G., Siddiqi, K., Thompson, P. M. (2009). Mathematical methods for diffusion MRI processing. *Neuroimage* 45:S111–S122.

Moakher, M. and Batchelor , P. G. (2006). *Visualisation and Processing of Tensor Fields*, chapter Symmetric Positive-Definite Matrices From Geometry to Applications and Visualisation, 291–295. Springer.

Wheeler-Kingshott, C. A., Barker, G. J., Steens, S. C., and Buchem, M. A. v. (2003). *Quantitative MRI of the Brain: measuring changes caused by disease*, chapter 7: the Diffusion of Water, pages 203–256. John Wiley & Sons Ltd.

Zhou, D., Dryden, I. L., Koloydenko, A., and Bai, L. (2008). A Bayesian method with reparameterisationfor diffusion tensor imaging. *Proceedings of SPIE Medical Imaging 2008: Image Processing, 69142J*. Edited by J. M. Reinhardt and J. P. W. Pluim.